arXiv:1609.04133v1 [hep-ph] 14 Sep 2016

A Discussion on Triangle Singularities in the $\Lambda_b \to J/\psi K^- p$ Reaction

Melahat Bayar[1,2], Francesca Aceti[2], Feng-Kun Guo[3] and Eulogio Oset[2]

[1]*Department of Physics, Kocaeli University, 41380, Izmit, Turkey*
[2]*Departamento de Física Teórica and IFIC,*
Centro Mixto Universidad de Valencia-CSIC,
Institutos de Investigación de Paterna,
Aptdo. 22085, 46071 Valencia, Spain
[3]*CAS Key Laboratory of Theoretical Physics, Institute of Theoretical Physics,*
Chinese Academy of Sciences, Beijing 100190, China

(Dated: September 15, 2016)

Abstract

We have analyzed the singularities of a triangle loop integral in detail and derived a formula for an easy evaluation of the triangle singularity on the physical boundary. It is applied to the $\Lambda_b \to J/\psi K^- p$ process via Λ^*-charmonium-proton intermediate states. Although the evaluation of absolute rates is not possible, we identify the χ_{c1} and the $\psi(2S)$ as the relatively most relevant states among all possible charmonia up to the $\psi(2S)$. The $\Lambda(1890)\,\chi_{c1}\,p$ loop is very special as its normal threshold and triangle singularities merge at about 4.45 GeV, generating a narrow and prominent peak in the amplitude in the case that the $\chi_{c1}\,p$ is in an S-wave. We also see that loops with the same charmonium and other Λ^* hyperons produce less dramatic peaks from the threshold singularity alone. For the case of $\chi_{c1}\,p \to J/\psi\,p$ and quantum numbers $3/2^-$ or $5/2^+$ one needs P- and D-waves, respectively, in the $\chi_{c1}\,p$, which drastically reduce the strength of the contribution and smooth the threshold peak. In this case we conclude that the singularities cannot account for the observed narrow peak. In the case of $1/2^+$, $3/2^+$ quantum numbers, where $\chi_{c1}\,p \to J/\psi\,p$ can proceed in an S-wave, the $\Lambda(1890)\,\chi_{c1}\,p$ triangle diagram could play an important role, though can neither assert their strength without further input from experiments and lattice QCD calculations.

I. INTRODUCTION

Triangle singularities in physical processes were introduced by Landau [1] and stem from Feynman diagrams involving three intermediate particles when the three particles can be placed simultaneously on shell and the momenta of these particles are collinear (parallel or antiparallel) in the frame of an external decaying particle at rest. In one of the cases (we call it parallel), two of the particles in the loop will go in the same direction and might fuse into other external outgoing particle(s) [2], so that the rescattering process can even happen as a classical process. In this case, the decay amplitude has a singularity close to the physical region[1] and, thus, can produce an enhancement. One of the classical cases would be given when the two on shell particles move in the same direction and with similar velocities. In the center-of-mass frame of the rescattering particles, these two particles would also be at rest and the triangle singularity is then located around the threshold.

One very successful example of effects of the triangle singularity was shown in the decay of $\eta(1405) \to \pi a_0(980)$ and $\eta(1405) \to \pi f_0(980)$ in Refs. [3, 4]. The second reaction breaks isospin symmetry. However, the process $\eta(1405) \to K^* \bar{K}$ followed by $K^* \to K\pi$ and the fusion of $K\bar{K} \to f_0(980)$ enhances drastically the rate of $\eta(1405) \to \pi f_0(980)$ relative to other isospin violating processes. Experimentally the ratio of rates for $\eta(1405) \to \pi^0 f_0(980) \to \pi^0\pi^+\pi^-$ and $\eta(1405) \to \pi^0 a_0(980) \to \pi^0\pi^0\eta$ is measured to be $(17.9 \pm 4.2)\%$ [5], a huge number for an isospin breaking magnitude. The work of [3, 4] was continued in [6] where the precise rates, as well as the shapes of the two reactions, are well described.

Another striking example of triangle singularities is the one discussed in Refs. [7, 8], where an interpretation for the "$a_1(1420)$" peak seen by the COMPASS Collaboration [9] is given in terms of a decay of the $a_1(1260)$ into $K^*\bar{K}$, followed by $K^* \to \pi K$ and fusion of $K\bar{K} \to f_0(980)$, with $\pi f_0(980)$ being the decay channel where the "$a_1(1420)$" peak is observed. A recent discussion of the effects of triangle singularities on other reactions in hadron physics can be found in Refs. [10–15].

With the discovery of the hidden charm pentaquark-like structures in the $\Lambda_b \to J/\psi K^- p$ reaction in the $J/\psi p$ spectrum [16, 17], the possibility that the narrow peak observed at 4.45 GeV might be due to a triangle singularity was immediately noted [18, 19]. Recently, the LHCb collaboration has reanalyzed [20] the data of the $\Lambda_b \to J/\psi\pi^- p$ decay [21] and found them consistent with the states reported in [16, 17]. The possibility that this is due to another triangle singularity is discussed in Ref. [22].

In Ref. [18] it is pointed out that the location of the $P_c(4450)$ structure coincides with the $\chi_{c1}p$ threshold and, more importantly, with the leading Landau singularity of the triangle diagram with the $\Lambda^*(1890)$, χ_{c1} and proton in the intermediate state. Such a diagram represents the following processes: the $\Lambda_b \to \Lambda^*(1890)\chi_{c1}$ is followed by the decay of $\Lambda^*(1890) \to K^- p$ and the proton, then, rescatters with the χ_{c1} into the $J/\psi p$ in the region where the invariant mass distribution shows up as a narrow sharp peak, which might cause a resonance-like structure as the $P_c(4450)$. However, the fact that one finds a singularity at a certain energy does not mean that one should see a peak in the reaction. The location of a triangle singularity is purely kinematic, yet the strength is controlled by dynamics as reflected by the coupling strengths of all of the three vertices involved. In this sense, the cases in the light meson sector discussed in Refs. [3, 4, 6–8] are nice examples of clearly showing the enhancement due to triangle singularities, since all involved couplings are relatively well

[1] It is in fact located away from the real energy axis, which prevents the physical amplitude from diverging, when a finite width is considered for the decaying particle in the triangle loop.

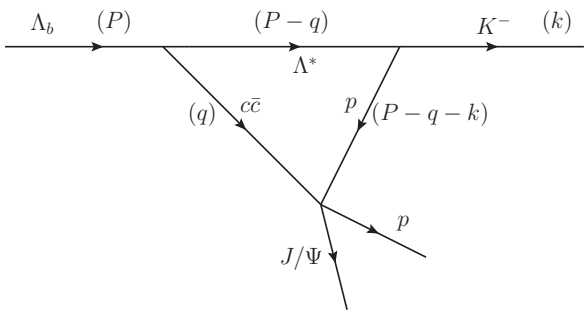

FIG. 1. Triangle diagram for $\Lambda_b \to J/\psi K^- p$ decay, where Λ^* stands for the different Λ^* considered in the analysis of [16, 21] and $c\bar{c}$ stands for different charmonium states. In brackets, the momenta of the corresponding lines are given.

known. In the case of the P_c, neither the weak decay rate of $\Lambda_b \to \Lambda^* \chi_{c1}$ nor the rescattering strength for $\chi_{c1}\, p \to J/\psi\, p$ is known and, thus, it is difficult to assert the importance of the triangle singularities. However, it is also obvious that triangle singularities need to be taken into account, unless the strength is so small that they can be safely neglected. At this point, we want to emphasize that the purpose of Refs. [18, 22] is not to show that the $P_c(4450)$ structure is due to triangle singularities instead of hadronic resonances, but to show that there exist such singularities around $m_{J/\psi p} = 4.45$ GeV, and their consequences need to be carefully explored.

In the present paper we shall make an exhaustive study of possible triangle singularities involving various Λ^* and charmonium intermediate states in the range of the $J/\psi p$ invariant mass in the $\Lambda_b \to J/\psi K^- p$ reaction. There can be many combinations of a Λ^* hyperon and a charmonium in the triangle diagram. However, as we shall see, since the condition for a triangle singularity to show up as a prominent enhancement in the relevant invariant mass distribution is rather strict (for recent discussions, see Refs. [13, 15, 18]), only a few of them deserve special attention, and the one discussed in Ref. [18] is the most special one. We will show them in the paper and discuss their possible repercussion in the $J/\psi p$ spectrum of the LHCb experiment.

II. DETAILED ANALYSIS OF THE TRIANGLE SINGULARITY

We are going to study the singularities that emerge from the diagram of Fig. 1. As in [18, 19] we assume that Λ_b decays first to a Λ^* and a charmonium state, the Λ^* decays into $K^- p$ and then the charmonium state and the p react to give the $J/\psi\, p$. Thus we have $J/\psi K^- p$ in the final state as in the experiment of [16].

The triangle singularities can be easily obtained by solving the Landau equation [1], as done in, e.g., Ref. [18]. Whether the solutions are located on the physical boundary, i.e., whether they can produce a prominent effect on the amplitude in the physically allowed region, is determined by the Coleman–Norton theorem [2]. It turns out that after fixing the masses of the proton and charmonium in the cases under consideration, only when the Λ^* mass is located in a small range there is a triangle singularity on the physical boundary. Since the mass region is small, the singularity is also close to the Λ^*–charmonium threshold (see, e.g., Refs. [13, 15, 18, 22]). Rather than using the Landau equation to get the singularities of

the amplitude for the diagram of Fig. 1, we find instructive to perform the loop integration of the three propagators explicitly. Let us consider the scalar three-point loop integral

$$I_1 = i \int \frac{d^4q}{(2\pi)^4} \frac{1}{(q^2 - m_{c\bar{c}}^2 + i\,\epsilon)\,[(P-q)^2 - m_{\Lambda^*}^2 + i\,\epsilon]\left[(P-q-k)^2 - m_p^2 + i\,\epsilon\right]}\,. \tag{1}$$

Since we are interested in the region where the Λ^* may be treated nonrelativistically, we can safely neglect the negative energy pole from the Λ^* propagator. We then perform the integral over q^0 analytically using the residue theorem and get, by taking the Λ_b at rest[2],

$$\begin{aligned} I_1 = \int \frac{d^3q}{(2\pi)^3} & \frac{1}{8\;\omega_X(\vec{q})\;E_\Lambda(\vec{q})\;E_p(\vec{k}+\vec{q})} \\ & \times \frac{1}{k^0 - E_p(\vec{k}+\vec{q}) - E_\Lambda(\vec{q})} \;\; \frac{1}{P^0 + \omega_X(\vec{q}) + E_p(\vec{k}+\vec{q}) - k^0} \\ & \times \frac{2\,P^0\omega_X(\vec{q}) + 2\,k^0 E_p(\vec{k}+\vec{q}) - 2\left[\omega_X(\vec{q}) + E_p(\vec{k}+\vec{q})\right]\left[\omega_X(\vec{q}\,) + E_p(\vec{k}+\vec{q}) + E_\Lambda(\vec{q}\,)\right]}{\left[P^0 - \omega_X(\vec{q}) - E_p(\vec{k}+\vec{q}) - k^0 + i\,\epsilon\right][P^0 - E_\Lambda(\vec{q}) - \omega_X(\vec{q}) + i\,\epsilon]}, \end{aligned} \tag{2}$$

where $\omega_X(\vec{q}) = \sqrt{m_{c\bar{c}}^2 + \vec{q}^{\,2}}$, $E_\Lambda(\vec{q}) = \sqrt{m_{\Lambda^*}^2 + \vec{q}^{\,2}}$, $E_p(\vec{k}+\vec{q}) = \sqrt{M_p^2 + (\vec{k}+\vec{q})^2}$, $P^0 = M_{\Lambda_b}$, and $k^0 = \sqrt{m_K^2 + \vec{k}^{\,2}}$.

We immediately observe that the poles of the propagators correspond to having pairs of intermediate particles on shell. The conditions for all the three intermediate particles to be on shell are

$$P^0 - E_\Lambda(\vec{q}) - \omega_X(\vec{q}) = 0\,, \tag{3}$$

$$P^0 - k^0 - \omega_X(\vec{q}) - E_p(\vec{k}+\vec{q}) = 0\,. \tag{4}$$

The other propagators do not lead to singularities, since a K^- cannot decay into a p and a Λ^* and $P^0 + \omega_X + E_p$ is always larger than k^0, and we thus have dropped the corresponding $i\,\epsilon$.

From Eqs. (3) and (4) we obtain

$$q_{\rm on} = \frac{\lambda^{1/2}(M_{\Lambda_b}^2, m_{\Lambda^*}^2, m_X^2)}{2\;M_{\Lambda_b}}\,, \tag{5}$$

$$\omega_X(q_{\rm on}) = \frac{M_{\Lambda_b}^2 + m_X^2 - m_{\Lambda^*}^2}{2\;M_{\Lambda_b}}\,, \tag{6}$$

$$E_\Lambda(q_{\rm on}) = \frac{M_{\Lambda_b}^2 + m_{\Lambda^*}^2 - m_X^2}{2\;M_{\Lambda_b}}\,, \tag{7}$$

where we have defined $\lambda(x,y,z) = x^2 + y^2 + z^2 - 2xy - 2yz - 2xz$.

In addition, we have from energy conservation for the process $\Lambda_b \to J/\psi K^- p$ with $J/\psi\; p$ with an invariant mass m_{23},

$$k^0 = \frac{M_{\Lambda_b}^2 + m_K^2 - m_{23}^2}{2\;M_{\Lambda_b}}\,, \quad k = \frac{\lambda^{1/2}(M_{\Lambda_b}^2, m_K^2, m_{23}^2)}{2\;M_{\Lambda_b}}\,. \tag{8}$$

[2] The expression can also be found in Eq. (19) of [23]. A simpler expression can be obtained if we neglect the negative energy poles for the $c\bar{c}$ and proton as well, which still retains the two relevant poles.

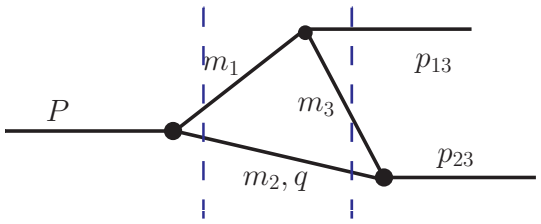

FIG. 2. A triangle diagram showing the notations used in the general discussion of triangle singularities, where m_i's denote the masses of the intermediate particles, and P, p_{13}, p_{23} correspond to the four-momenta of the external particles. The two dashed vertical lines correspond to the two relevant cuts.

Then Eq. (4) leads immediately to

$$\frac{m_{23}^2 + m_{\Lambda^*}^2 - m_K^2 - m_X^2}{2\ M_{\Lambda_b}} - \sqrt{m_p^2 + (\vec{q} + \vec{k})^2} = 0\,, \tag{9}$$

which is the equation providing the singularities of the integrand of the loop integral in Eq. (3). However, a singularity of the integrand is not necessarily the singularity of the integral. If we can deform the integration contour in the complex plane to avoid the singularity, the integral would be regular. In the following two cases, one cannot deform the contour and a singularity develops: when the singularity of the integrand is located at the endpoint of the integration, and when two or more singularities of the integrand pinch the contour. They correspond to the cases of endpoint and pinch singularities, respectively. We now apply this knowledge to the problem at hand.

We notice that, in order to analyze the singularity structure, it is sufficient to focus on the following integral:

$$\begin{aligned} I(m_{23}) &= \int d^3q \, \frac{1}{\left[P^0 - \omega_1(\vec{q}) - \omega_2(\vec{q}) + i\,\epsilon\right]\left[E_{23} - \omega_2(\vec{q}) - \omega_3(\vec{k} + \vec{q}) + i\,\epsilon\right]} \\ &= 2\,\pi \int_0^\infty dq \ \frac{q^2}{P^0 - \omega_1(q) - \omega_2(q) + i\,\epsilon} f(q)\,, \end{aligned} \tag{10}$$

where, in the rest frame of the decaying particle and with the more general notation as labelled in Fig. 2, $\omega_{1,2}(q) = \sqrt{m_{1,2}^2 + q^2}$, $\omega_3(\vec{q} + \vec{p}_{13}) = \sqrt{m_3^2 + (\vec{q} + \vec{p}_{13})^2}$, $E_{23} = P^0 - p_{13}^0$, and

$$f(q) = \int_{-1}^{1} dz \, \frac{1}{E_{23} - \omega_2(q) - \sqrt{m_3^2 + q^2 + k^2 + 2\,q\,k\,z} + i\,\epsilon}\,, \tag{11}$$

where $k = |\vec{p}_{13}| = \sqrt{\lambda(M^2, m_{13}^2, m_{23}^2)}/(2M)$, with $M = \sqrt{P^2}$ and $m_{13,23} = \sqrt{p_{13,23}^2}$, and $q = |\vec{q}|$. The integral $I(m_{23})$ is in fact a function of all involved masses and external momenta, and here we only show m_{23} since we will discuss the singularities in this variable. It becomes clear that we need to analyze the singularity structure of a double integration: one over q and one angular integration over z. The two factors in the denominator of the integrand of $I(m_{23})$ correspond to the two cuts depicted in Fig. 2. The cut crossing particles 1 and 2 provides a pole of the integrand of $I(m_{23})$ given by

$$P^0 - \omega_1(\vec{q}) - \omega_2(\vec{q}) + i\,\epsilon = 0\,, \tag{12}$$

which is just Eq. (3) by identifying $m_1 = m_{\Lambda^*}$ and $m_2 = m_{c\bar{c}}$. However, we have kept the $i\,\epsilon$ here explicitly, which is important to determine the singularity locations in the complex-q plane. The pertinent solution is

$$q_{\rm on+} = q_{\rm on} + i\,\epsilon \quad \text{with} \quad q_{\rm on} = \frac{1}{2M}\sqrt{\lambda(M^2, m_1^2, m_2^2)}\,. \tag{13}$$

The function $f(q)$ has endpoint singularities, which are logarithmic branch points, given when the denominator of the integrand vanishes for z taking the endpoint values ± 1, i.e., the solutions of

$$E_{23} - \omega_2(q) - \sqrt{m_3^2 + q^2 + k^2 \pm 2\,q\,k} + i\,\epsilon = 0\,, \tag{14}$$

which is just Eq. (4) by identifying $m_2 = m_{c\bar{c}}$ and $m_3 = m_p$. The $+$ and $-$ signs correspond to $z = +1$ and -1, i.e., the situations for the momentum of particle 2 to be anti-parallel and parallel to the momentum of the (2,3) system in the frame with $\vec{P} = 0$, respectively. These endpoint singularities of $f(q)$ provide logarithmic branch point singularities to the integrand of $I(m_{23})$, in addition to the pole given by the first cut. Whether they induce singularities in $I(m_{23})$ needs to be further analyzed and we do it in the following.

For $z = -1$, Eq. (14) has two solutions:

$$q_{a+} = \gamma\,(v\,E_2^* + p_2^*) + i\,\epsilon\,, \qquad q_{a-} = \gamma\,(v\,E_2^* - p_2^*) - i\,\epsilon\,, \tag{15}$$

where we have defined

$$\begin{aligned} v &= \frac{k}{E_{23}}\,, & \gamma &= \frac{1}{\sqrt{1-v^2}} = \frac{E_{23}}{m_{23}}\,, \\ E_2^* &= \frac{1}{2m_{23}}\left(m_{23}^2 + m_2^2 - m_3^2\right), & p_2^* &= \frac{1}{2m_{23}}\sqrt{\lambda(m_{23}^2, m_2^2, m_3^2)}\,. \end{aligned} \tag{16}$$

It is easy to realize that E_2^* and p_2^* are the energy and the magnitude of the 3-momentum of particle-2 in the center-of-mass frame of the (2,3) system, v is the magnitude of the velocity of the $(2,3)$ system in the rest frame of the decaying particle and γ is the Lorentz boost factor. Therefore, the two solutions given above correspond to the momentum of particle-2 in the rest frame of the decaying particle in different kinematic regions, which will be discussed later.

For $z = 1$, the two solutions of Eq. (14) are:

$$q_{b+} = \gamma\,(-v\,E_2^* + p_2^*) + i\,\epsilon\,, \qquad q_{b-} = -\gamma\,(v\,E_2^* + p_2^*) - i\,\epsilon\,. \tag{17}$$

The second one, q_{b-} is irrelevant since it is always negative when $\epsilon = 0$, and is never realized in the integral on the momentum modulus in Eq. (10). It might be worthwhile to emphasize that all of $q_{a\pm}$ and $q_{b\pm}$ are singularities of the integrand of $I(m_{23})$ simultaneously. However, depending on the value of m_{23} (for real m_{23}), either $\lim_{\epsilon\to 0}(q_{a-})$ or $\lim_{\epsilon\to 0}(q_{b+})$, but not both, is positive and appears in the relevant integration range of q from 0 to $+\infty$. These two cases are shown in Fig. 3 and Fig. 4, respectively.

Let us discuss Fig. 3 first. In the integration range of q, the integrand has three relevant singularities: a pole $q_{\rm on+}$ and two logarithmic branch points $q_{a\pm}$. Their locations are determined by kinematics. It can happen that all of them are located at different positions, and one can deform the integration path freely as long as it does not hit any singularity of the integrand. One such path is shown as the dashed line segments in Fig. 3 (a). In such a kinematic region, $I(m_{23})$ is analytic. Since q_{a-} is in the lower half of the complex-q plane

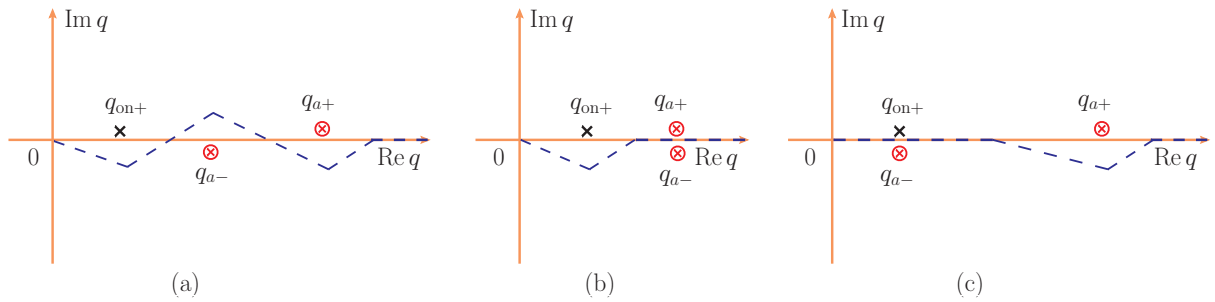

FIG. 3. Pertinent singularities of the integrand of $I(m_{23})$ when $\lim_{\epsilon\to 0}(q_{a-})$ is positive. (a) is for the case without any pinching, (b) shows the case when the integration path is pinched between q_{a+} and q_{a-}, which gives the two-body threshold singularity, and (c) is for the case when the pinching happens between $q_{\rm on+}$ and q_{a-}, which gives the triangle singularity. The dashed lines correspond to possible integration paths.

while $q_{\rm on+}$ and q_{a+} are in the upper half plane, it could happen that the integration path is pinched between q_{a-} and one of $q_{\rm on+}$ and q_{a+} or even both of them. Then one cannot deform the integration path away from the singularities of the integrand and $I(m_{23})$ will be nonanalytic as well. If the integration path is pinched between q_{a-} and q_{a+}, as shown in Fig. 3 (b), which happens when $m_{23} = m_2 + m_3$ or $p_2^* = 0$, one gets the normal two-body threshold singularity which is a square-root branch point. If the integration path is pinched between q_{a-} and $q_{\rm on+}$, as shown in Fig. 3 (c), one gets the triangle singularity or anomalous threshold which is a logarithmic branch point. Therefore, the condition for a triangle singularity to emerge is given mathematically by

$$\lim_{\epsilon\to 0}(q_{\rm on+} - q_{a-}) = 0\,. \tag{18}$$

This is only possible when all three intermediate particles are on shell and meanwhile $z = -1$, $\omega_1(q_{\rm on}) - p_{13}^0 - \sqrt{m_3^2 + (q_{\rm on} - k)^2} = 0$ (it has another solution q_{a+}). The location of the triangle singularity in the variable m_{23} is found by solving the above equation. It could also happen that both $q_{\rm on+}$ and q_{a+} pinch the integration path with q_{a-} at the same time, and then the triangle singularity coincides with the normal threshold at $m_{23} = m_2 + m_3$. Yet, although this requires a very special kinematic configuration, it does happen at $M_{J/\psi p} \simeq 4.45$ GeV for the $\Lambda^*(1890)$–χ_{c1}–proton diagram contribution to the $\Lambda_b \to KJ/\psi p$ as discussed in Ref. [18].

It is important to understand the kinematic region where the triangle singularity can occur. Since q_{a-} is the singularity of $f(q)$ at the endpoint $z = -1$, the momentum of particle-3 in the rest frame of the decaying particle is thus $\vec{p}_3 = -\vec{q} - \vec{p}_{13} = (k - q)\hat{q}$, where $\hat{q}$ stands for the unit vector along the direction of $\vec{q}$. From Eqs. (15) and (16), it is easy to see that $k > \lim_{\epsilon\to 0}(q_{a-})$ for $m_{23} \geq m_2 + m_3$. Thus, particles 2 and 3 move in the same direction in this reference frame. Another condition for q_{a-} to be relevant becomes clear by checking the expression of q_{a-} in Eq. (15), which is the Lorentz boost of the momentum of particle-2 from the center-of-mass frame of the (2,3) system to the rest frame of the decaying particle. The negative sign in front of p_2^* in Eq. (15) means that the direction of motion of particle-2 in the center-of-mass frame of the $(2, 3)$ system is opposite to the one in the rest frame of the decaying particle, while the direction of motion of particle-3 is the same in both reference frames. This implies that particle-3 moves faster than particle-2 in the latter

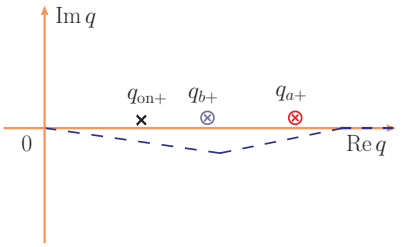

FIG. 4. Pertinent singularities of the integrand of $I(m_{23})$ when $\lim_{\epsilon\to 0}(q_{b+})$ is positive.

reference frame. Therefore, the triangle singularity happens only when particle-3 moves along the same direction as particle-2, and has a larger velocity in the rest frame of the decaying particle. This, together with having all intermediate particles on their mass shells, gives the condition for having a triangle singularity. One can realize that this is in fact the Coleman–Norton theorem [2]: the singularity is on the physical boundary if and only if the diagram can be interpreted as a classical process in space-time.

For given m_2, m_3 and invariant masses for external particles, one can also work out the range of m_1 where the triangle singularity shows up, as well as the range of the triangle singularity in m_{23}. For $q_{\rm on}$ and q_{a-} (taking $\epsilon = 0$) taking values in their physical regions, one needs to have $m_1 \leq M - m_2$ and $m_{23} \geq m_2 + m_3$. Using Eq. (18), we find that when

$$m_1^2 \in \left[\frac{M^2 m_3 + m_{13}^2 m_2}{m_2 + m_3} - m_2 m_3\,,\ \ (M - m_2)^2\right], \tag{19}$$

$I(m_{23})$ has a triangle singularity, and it is within the range

$$m_{23}^2 \in \left[(m_2 + m_3)^2,\ \ \frac{M m_3^2 - m_{13}^2 m_2}{M - m_2} + M m_2\right]. \tag{20}$$

These are in fact the ranges discussed in Refs. [18, 22] derived from the point of view of the Coleman–Norton theorem.

The kinematic region where particle-2 moves faster than particle-3 but in the same direction corresponds to the case that the three-momentum of the on shell particle-2 takes the value of q_{a+}. One then has $\lim_{\epsilon\to 0}(q_{a+} - q_{a-}) > 0$ (it would be equal to 0 if the two particles move with the same speed in the rest frame of the decaying particle), and $I(m_{23})$ has no singularity. From the point of view of the Coleman–Norton theorem [2], particle-3 emitted from the decay of particle-1 cannot catch up with particle-2 so that the rescattering between them in the triangle diagram cannot be interpreted as a classical process. This case corresponds to Fig. 3 (a).

There is the possibility that $q_{a-} < 0$ (here and in the following when we talk about the sign or relative size of $q_{a\pm}$ and $q_{b\pm}$, ϵ takes the value of 0) and, thus, this solution is unphysical for on-shell intermediate particles. In this case, solving numerically Eq. (9) with $\vec{q}$ and $\vec{k}$ in opposite directions will give only one positive q solution, which, by necessity, is q_{a+}. Note that $q_{a-} < 0$ means $q_{b+} = -q_{a-} > 0$, so that q_{b+} is in the physical range of q. We show this case in Fig. 4, where only the positive singularities of the integrand, which are the ones in the physical range of q for on-shell intermediate particles, are depicted. Since $q_{a-} < 0$ in this case, and $q_{b-} < 0$, and furthermore $q_{\rm on+}$, q_{a+} and q_{b+} are on the same side of

$c\bar{c}$	Most relevant range of M_{Λ^*} (MeV)	Range of triangle singularity (MeV)
η_c	[2226, 2639]	[3919, 4283]
J/ψ	[2151, 2523]	[4035, 4366]
χ_{c0}	[1949, 2205]	[4353, 4588]
χ_{c1}	[1887, 2109]	[4449, 4654]
χ_{c2}	[1858, 2063]	[4494, 4686]
h_{c1}	[1878, 2094]	[4464, 4664]
$\eta_c(2S)$	[1806, 1983]	[4575, 4741]
$\psi(2S)$	[1774, 1933]	[4624, 4775]

TABLE I. For each charmonium, the triangle singularity produces prominent effects if the Λ^* mass takes a value within the the range given in the second column and the singularity range is shown in the last column correspondingly. As seen from Eq. (20), the first number in each row of the last column corresponds to the threshold of the proton and the corresponding charmonium.

the $\mathrm{Re}\, q$ axis, no pinching can occur and, hence, none of these singularities of the integrand turns into a singularity of the integral $I(m_{23})$. The condition for $q_{a-} < 0$ is $p_2^* > v\, E_2^*$, i.e., the magnitude of velocity of particle-2 in the (2,3) center-of-mass frame (which is equal to the one for particle-3) is larger than the velocity of the $(2,3)$ system in the rest frame of the initial particle. It implies that particle-2 and particle-3 move in opposite directions in the latter frame and thus particle-3, emitted from the decay of particle-1, which moves also opposite to particle-2 in the rest frame of the initial particle, cannot rescatter with particle-2 in a classical picture with energy-momentum conservation, in accordance with the conclusion of Ref. [2].

III. RESULTS

Now let us turn to the problem of possible triangle singularities contributing to the $\Lambda_b \to K^- J/\psi\, p$ from triangle diagrams with a Λ^* hyperon, a charmonium and a proton as the intermediate states. The Λ^* states considered in the fit of data by the LHCb Collaboration include [16]: $\Lambda(1405)$, $\Lambda(1520)$, $\Lambda(1600)$, $\Lambda(1670)$, $\Lambda(1690)$, $\Lambda(1800)$, $\Lambda(1810)$, $\Lambda(1820)$, $\Lambda(1830)$, $\Lambda(1890)$, $\Lambda(2100)$, $\Lambda(2110)$, $\Lambda(2350)$, $\Lambda(2585)$ which as seen in [24] couple to $K^- p$. As to the charmonium states we take $\eta_c(1S)$, J/ψ, $\chi_{cJ}(1P)$ $(J = 0, 1, 2)$, $h_c(1P)$, $\eta_c(2S)$, and $\psi(2S)$. From the discussion in the preceding section and Eqs. (19) and (20) we can see which is the mass range allowed for the Λ^* particles, for a certain charmonium state, in order to have a triangle singularity. In Table I, we give these values as well as the range of the corresponding invariant mass of the (2,3) system ($J/\psi\, p$) at which the triangle singularity appears. We can then select the Λ^*'s fulfilling these requirements, that will be shown later after the following discussions on the experimental production rates and relevance of these different charmonia.

As discussed in the preceding section, we expect to have contributions from the triangle singularity, which is a logarithmic branch point, and from the two-body threshold, which is a square-root branch point. While the first one does indeed lead to an infinite contribution if all of the involved masses take real values, the second one gives a finite contribution. Yet, the triangle singularity turns into a finite contribution because particle-1 necessarily decays

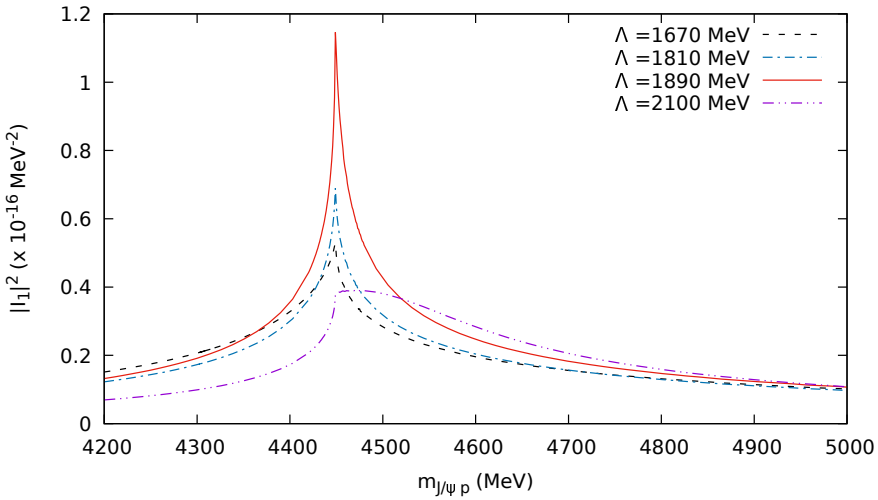

FIG. 5. The value of $|I_1|$ (Eq. (3)) for $\Lambda^* \chi_{c1}$ with a width $\Gamma = 100$ MeV for the hyperon.

into particle-3 and the external (1,3) particle(s) (the K^- in the problem at hand), providing a width to particle-1 and, hence, replacing the $i\,\epsilon$ by $i\,\Gamma/2$ ($i\,\Gamma_{\Lambda^*}/2$ in the present case). Of course, the Λ^* has more decay channels than just the one into particle-3 plus the $(1,3)$ system and the full width needs to be used for Γ. Now the two singularities of the integrand $q_{\rm on+}$ and q_{a-} that were pinching before in Fig. 3 (c) are now separated such that we obtain a finite result for the integral $I(m_{23})$, and for the decay amplitude involving the triangle loop as well, which has memory of the singularity and produces an enhancement in this integral.

In what follows we would like to discuss which charmonium states are relevant from a physical point of view.

We can have an idea of strength of the $\Lambda_b \to \Lambda c\bar{c}$ for the different charmonium statethe s by looking at the related rates of $B \to c\bar{c}\bar{K}$. In Table II we collect the rates given by the PDG in all these cases. This means that one can neglect the χ_{c2} and h_{c1} cases. The χ_{c0} has also a factor three smaller rate. On the other hand, the $\chi_{c0}\,p \to J/\psi\,p$ amplitude is of the same order of magnitude as the $\chi_{c1}\,p \to J/\psi\,p$ [18]. Altogether, we have about a factor three reduction in the triangle diagram and we can dismiss this term as subdominant. The $\eta_c(2S)$ has $J^P = 0^-$ and the $c\bar{c}$ with 0^- has to be converted into 1^- for the J/ψ in the $\eta_c(2S)\,p \to J/\psi\,p$ reaction and this implies a spin flip of the charmed quarks. This should be much suppressed by heavy quark spin symmetry.

Finally, the $\psi(2S)$ has a $B \to c\bar{c}\,\bar{K}$ branching fraction about 1.5 times bigger than the χ_{c1}. The $\psi(2S)\,p \to J/\psi\,p$ amplitude has two sources, one from soft gluon exchange, that would be suppressed for the $\psi(2S)\,p \to J/\psi\,p$ with respect to the $\chi_{c1}\,p \to J/\psi\,p$, because of the smaller overlap between the radial wave functions, and another source is given by the subsequent exchange of D^* or D as done in Refs. [26, 27]. In this latter case, we do not find a strong reason why the latter mechanism should be much reduced with respect to the case of $\chi_{c1}\,p \to J/\psi\,p$.

We also admit that all the $c\bar{c}\,p \to J/\psi\,p$ amplitudes are OZI suppressed and that, at this moment we have no elements to evaluate the strength of these amplitudes nor the $\Lambda_b \to \Lambda^*\,c\bar{c}$ ones. Hence, the global strength of these singularities is unknown at present.

Let us first discuss the χ_{c1} intermediate charmonium and assume the $\chi_{c1}\,p$ in the $\chi_{c1}\,p \to J/\psi\,p$ amplitude to be in an S-wave and, similarly, we do not pay attention to the particular

$c\bar{c}$	$BR(B \to c\bar{c}\bar{K})$
χ_{c0}	$1.5 \cdot 10^{-4}$ (neutral B) $1.3 \cdot 10^{-4}$ (charged B)
χ_{c1}	$4.0 \cdot 10^{-4}$ (neutral B) $4.6 \cdot 10^{-4}$ (charged B)
χ_{c2}	$< 1.5 \cdot 10^{-5}$
h_{c1}	$< 3.8 \cdot 10^{-5}$
$\eta_c(2S)$	$3.4 \cdot 10^{-4}$
$\psi(2S)$	$6.26 \cdot 10^{-4}$

TABLE II. Branching ratios for $B \to c\bar{c}\bar{K}$ [24]. Here we only quote the central values.

structure of the other vertices (this will be done in the next section). We plot the contribution to $|I_1|^2$ from a selected choice of the Λ^* states discussed above in Fig. 5. We can see that all of them peak around $m_{23} = 4450$ MeV, which is the $\chi_{c1}\,p$ threshold. The largest strength, with the sharpest shape, comes from the $\Lambda(1890)$, which is the one discussed in Ref. [18]. We should note that in this case the threshold and the triangle singularities merge, and we attribute the prominent role of this Λ^* state to this feature.

The cusp structure in the curve for the $\Lambda(1670)$ comes from the threshold singularity (see in the second column of Table I that this mass is far outside the range of the Λ^* mass for having a triangle singularity). The peak of the $\Lambda(1810)$ is sharper, for, even if the Λ^* mass is outside the range of the triangle singularity (see Table I), it is not too far away, but the most relevant factor in the structure is the threshold singularity.

The case of the $\Lambda(2100)$ is special: indeed, as seen in Table I, this mass is inside the range of the triangle singularities and we can easily see, using Eq. (18), that it appears at 4592 MeV. Hence, the structure of I_1 for this Λ^* state shows a bump, in addition to the normal threshold cusp, around that energy, as a consequence of the smearing of the triangle singularity by the width of the Λ^*, as discussed before.

For the $\psi(2S)$ case, one finds a similar pattern but we shall discuss in more detail this case, by comparing it to the χ_{c1} case, in the next section.

IV. DETAILED ANALYSIS OF THE S AND P-WAVE AMPLITUDES FOR χ_{c1} AND $\psi(2S)$ AND $\Lambda(1890)$

In this section, we will discuss the structure of triangle loops involving the $\Lambda(1890)$ and the χ_{c1} or $\psi(2S)$, taking into account the necessary operator structures.

Let us look at Fig. 1. Since the spin of the $\Lambda(1890)$ is 3/2, the $\Lambda_b \to \Lambda(1890)\,c\bar{c}$ vertex can be accommodated with the operator $\vec{S}^\dagger \cdot \vec{\epsilon}$, with $\vec{S}^\dagger$ the spin transition operator from a spin-1/2 to spin-3/2 state and $\vec{\epsilon}$ the polarization of the spin-1 charmonium. The $\Lambda(1890) \to K^- p$ vertex is of the type $\vec{S} \cdot \vec{k}$. Finally in the $c\bar{c}\; p \to J/\psi\; p$ we have several situations:

1. The quantum numbers of the $J/\psi\, p$, those for the $P_c(4450)$, are $J^P = 3/2^-$:

   (a) $c\bar{c} = \chi_{c1}$: This requires a P-wave in the $\chi_{c1}\, p$ system which can be accommodated with the operator $(\vec{\sigma} \cdot \vec{q}^{\,*}\;\; \vec{\epsilon} \cdot \vec{\epsilon}\,')/m_p$, where $\vec{\sigma}$ are the Pauli matrices, $\vec{q}^{\,*}$ is the

momentum of χ_{c1} in the loop in the $\chi_{c1}\,p$ center-of-mass frame, and $\vec{\epsilon}$ and $\vec{\epsilon}\,'$ are the polarization vectors of the χ_{c1} and J/ψ respectively).

(b) $c\bar{c} = \psi(2S)$: This requires an S-wave in both the $\psi(2S)\,p$ and $J/\psi\,p$ channels. We thus take a constant, which is normalized to the former amplitude at a scale of the q^* momentum equal to the mass of the proton.

2. The quantum numbers of the $J/\psi\,p$ are $J^P = 1/2^+$ or $3/2^+$:

(a) $c\bar{c} = \chi_{c1}$: In this case the $\chi_{c1}p$ system is in an S-wave and the $J/\psi p$ in a P-wave. The roles of the χ_{c1} and J/ψ are reverted with respect to the case (1.a) and we then have the same amplitude as in the case of (1.a), interchanging the momenta of the χ_{c1} and the J/ψ, hence $(\vec{\sigma}\cdot\vec{p}^{\,*}\,\vec{\epsilon}\cdot\vec{\epsilon}\,')/m_p$, with $\vec{p}^{\,*}$ the momentum of the J/ψ in the $J/\psi\,p$ center-of-mass frame.

(b) $c\bar{c} = \psi(2S)$: this requires a P-wave in both the $\psi(2S)p$ and $J/\psi p$ systems, and will not play a role in the discussion.

In the case (1.a) the spin-momentum structure of the integrand of the triangle diagram is then

$$\vec{S}\cdot\vec{k}\,\vec{S}^{\dagger}\cdot\vec{\epsilon}\,\vec{\sigma}\cdot\vec{q}^{\,*}\,\vec{\epsilon}\cdot\vec{\epsilon}\,'. \tag{21}$$

Using the Lorentz boost formula in the compact form as given in Ref. [28], we can express $\vec{q}^{\,*}$ in the center-of-mass frame of the $J/\psi\,p$ (or $\chi_{c1}\,p$) in terms of the quantities in the rest frame of the Λ_b, where the loop integral was evaluated in former sections. Noticing that the former frame is moving with a momentum $-\vec{k}$ in the latter frame, we get

$$\vec{q}^{\,*} = \left[\left(\frac{E_R}{m_{23}} - 1\right)\,\frac{\vec{q}\cdot\vec{k}}{\vec{k}^2} + \frac{q^0}{m_{23}}\right]\vec{k} + \vec{q}, \tag{22}$$

where m_{23} is the invariant mass of the $J/\psi\,p$ system, $E_R = \sqrt{m_{23}^2 + \vec{k}^2}$ and $q^0 = \sqrt{m_{\chi_{c1}}^2 + \vec{q}^{\,2}}$, with $\vec{k}$ the momentum of the kaon and $\vec{q}$ the momentum of the χ_{c1} in the loop. Next we take into account that, since $\vec{k}$ is the only vector not integrated in the integral of I_1, we can write

$$\int d^3q\,A(\vec{q})q_i = k_i\int d^3\vec{q}\,A(\vec{q})\,\frac{\vec{k}\cdot\vec{q}}{\vec{k}^2}\,, \tag{23}$$

where $A(\vec{q})$ stands for the rest part of the loop integrand. This means that, because of the P-wave between the χ_{c1} and proton, $\vec{q}^{\,*}$ in Eq. (21) in the integrand of the triangle loop can be replaced by the following factor:

$$\vec{k}\left(\frac{E_R\,\vec{q}\cdot\vec{k}}{m_{23}\,\vec{k}^2} + \frac{q^0}{m_{23}}\right). \tag{24}$$

With the following integral

$$I_2 = \int\frac{d^3\vec{q}}{(2\pi)^3}\left(\frac{E_R\,\vec{q}\cdot\vec{k}}{m_{23}\,\vec{k}^2} + \frac{q^0}{m_{23}}\right)\times(\text{integrand of } I_1)\,, \tag{25}$$

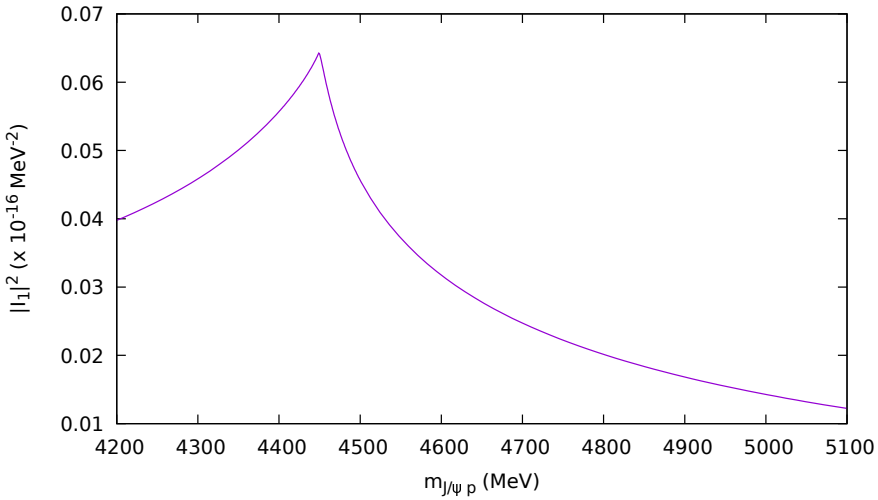

FIG. 6. The value of $|I_2|^2$ for P-wave $\Lambda(1890)\chi_{c1}$. A constant width of $\Gamma = 100$ MeV is used for the $\Lambda(1890)$.

we can get the amplitude T for the $\Lambda_b \to K^- J/\psi\, p$ decay process via the pertinent triangle diagram. After carrying the sum and average of the polarizations given in Eq. (21), we obtain the factor $2\,\vec{k}^4/(3\,m_p^2)$. Hence, we obtain for the case (1.a)

$$|T_{(1.a)}|^2 = \frac{2\,\vec{k}^4}{3\,m_p^2}|I_2|^2\,. \tag{26}$$

In the case (2.a), we have the same spin-momentum factor as Eq. (21) substituting $\vec{\sigma}\cdot\vec{q}^{\,*}$ by $\vec{\sigma}\cdot\vec{p}^{\,*}$, and the final result is

$$|T_{(2.a)}|^2 = \frac{2\,\vec{k}^2\,\vec{p}^{\,*\,2}}{3\,m_p^2}|I_1|^2\,. \tag{27}$$

In the case (1.b), the expression of Eq. (21) is substituted by $\vec{S}\cdot\vec{k}\,\vec{S}^{\dagger}\cdot\vec{\epsilon}\,\vec{\epsilon}\cdot\vec{\epsilon}\,'$, and we obtain

$$|T_{(1.b)}|^2 = \frac{2\,\vec{k}^2}{3}|I_1|^2\,. \tag{28}$$

The pre-factors of momentum are numerically very similar and we may eliminate them for the discussion and hence use only the $|I_{1,2}|^2$ part. The results for the cases (1.a) and (1.b) are shown in Figw. 6 and 7, respectively; the result for the case (2.a) has already been given as the solid curve in Fig. 5.

We can see that, in the case of $3/2^-$ for the $J/\psi\, p$ final states and $\chi_{c1}\, p$, which requires a P-wave, the amplitude is very much suppressed with respect to the case where one has the $c\bar{c}\, p$ in S-wave. This is natural since the singularity appears when putting the $\chi_{c1}\, p$ on shell and at threshold, where the P-wave factor vanishes. We can see that the strength at the peak is about 20 times smaller than the one in the S-wave case. We also see that the S-wave structure is very much peaked and narrow, while the one of the P-wave has a "background" below the peak, accumulating more strength than the peak. Also the shape is too broad to associate it to the observed narrow pentaquark in the experiment.

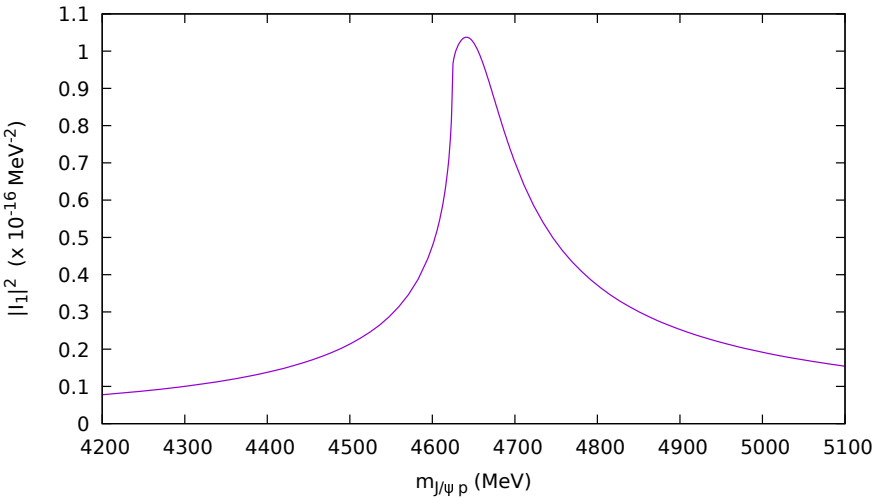

FIG. 7. The value of $|I_1|^2$ for S-wave $\Lambda(1890)\psi(2S)$. A constant width of $\Gamma = 100$ MeV is used for the $\Lambda(1890)$.

There is another factor to take into account. In this case the contribution of the $\psi(2S)\, p$, which proceeds via an S-wave, would give us a narrow peak around 4624 MeV, much stronger than the one provided by the P-wave $\chi_{c1}\, p$, assuming the rescattering strengths are comparable. An inspection of the experimental data shows that the $J/\psi p$ invariant mass distribution in this region is flat. These arguments lead to the conclusion that, if the narrow $J/\psi\, p$ structure has quantum numbers $3/2^-$, one of the choices in the experimental analysis, the triangle singularities due to $\Lambda^*\, c\bar{c}\, p$ intermediate states cannot play an important role in the decay $\Lambda_b \to K^- J/\psi\, p$.

The other quantum numbers preferred in the current experimental analysis for the narrow state are $5/2^+$. In this case, one needs a D-wave in $\chi_{c1}\, p$ and the situation is worse. We have checked that numerically but there is no need to discuss it.

We pass now to discuss the possibility that the $J/\psi\, p$ system in the narrow structure takes the quantum numbers $1/2^+$ or $3/2^+$. In this case the $\chi_{c1}\, p$ amplitude proceeds via an S-wave and we would have the situation shown as the solid curve in Fig. 5. The peak is narrow enough and located at the right position. Furthermore, the $\Lambda(1890)\, \chi_{c1}\, p$ triangle diagram reinforces by merging the triangle singularity with the normal $\chi_{c1}\, p$ threshold at 4.45 GeV, which makes the peak more prominent than in the other cases. This was pointed out in Ref. [18], which tried to draw attention to the complications of interpreting the $P_c(4450)$.[3] In this case, the contribution from the $\psi(2S)$ intermediate state would proceed with $\psi(2S)\, p$ in a P-wave and would be drastically reduced with respect to the one shown in Fig. 7.

V. CONCLUSIONS

We have analyzed in detail when the singularities of the triangle amplitude appear with a different formalism than the one normally used, which allows for a complementary understanding of their origin, as well as for an easy evaluation of the singularities. They are

[3] In Ref. [18], the authors did not claim that the $P_c(4450)$ is due to the triangle singularity. On the contrary, a method discriminating the true resonance explanation from the $\Lambda(1890)\, \chi_{c1}\, p$ triangle singularity was proposed.

generated by a genuine triangle singularity or from threshold effects. We applied the method to the $\Lambda_b \to J/\psi K^- p$ decay and discussed all possible triangle singularities that might affect the $J/\psi\, p$ mass distribution from a triangle diagram involving a charmonium, a proton and a Λ^* hyperon. We stressed that, should the $\chi_{c1}\, p$ in the $\chi_{c1}\, p \to J/\psi\, p$ amplitude be in an S-wave, the intermediate $\chi_{c1}\, \Lambda(1890)$ pair plays a very special role, since the threshold and triangle singularities merge. In many of the other cases we see that they do not develop a triangle singularity, but the threshold cusp is always present as it should.

We also made a study of the different cases using dynamical features and some phenomenology and concluded that the relevant singularities, if strong enough to be observable, should develop from $\chi_{c1}\, p$ and $\psi(2S)\, p$ intermediate states. Then we saw that in the case of $J^P = \frac{3}{2}^-,\ \frac{5}{2}^+$ for the narrow P_c, as presently favoured by the experiment, the $\chi_{c1}\, p \to J/\psi\, p$ transition requires $L = 1$ in $\chi_{c1}\, p$ in the first case and $L = 2$ in the second. This feature smoothens very much the peak to the point that the interpretation of the experimental peak on this singularity runs into obvious inconsistencies. In this case a singularity stemming from the $\psi(2S)\, p$ intermediate state proceeds with $\psi(2S)\, p$ in an S-wave, located at around 4624 MeV in the $J/\psi\, p$ invariant mass. The flat distribution in the experimental data would mean that the $\psi(2S)\, p \to J/\psi\, p$ is not strong enough to make the triangle singularity observable. These considerations lead us to conclude that if the narrow $P_c(4450)$ has quantum numbers $J^P = \frac{3}{2}^-,\ \frac{5}{2}^+$, reported as the preferable quantum numbers in the LHCb analysis of their data, it would have an origin other than a triangle singularity from the Λ^*–charmonium–proton intermediate states.

Should this narrow peak correspond to $J^P = \frac{1}{2}^+$ or $\frac{3}{2}^+$, the $\chi_{c1}\, p$ can proceed in S-wave. In such a case we could show that the $\chi_{c1}\, p$ intermediate state and the $\Lambda(1890)$ would be favoured over the other possible $\Lambda^*\, c\bar{c}\, p$ intermediate states. This was because the mass of the $\Lambda(1890)$ makes the triangle and threshold singularities merge at the same energy. We also saw that in this case the contribution of the other Λ^* states could provide a relevant contribution due to the threshold singularity. We admit that the $\chi_{c1}\, p \to J/\psi\, p$ amplitude is OZI suppressed, and we do not know its strength. However, we also notice that the NPLQCD Collaboration recently reported possible existence of charmonium-nucleus bound states in their lattice QCD calculation even when extrapolated to the physical pion mass [29].

The spin and parity assignment to the two P_c structures reported in Ref. [16] is not fully settled and further work continues in the collaboration to be more assertive in the near future[4]. Further stimulus for this task stems from the recent work [30], which shows that from the $K^- p$ and $J/\psi\, p$ invariant mass distributions alone, one cannot asset the spin and parity of the two P_c structures, nor the need for the broad $P_c(4380)$ state. The work also shows that contact terms, that turn out to be negligible in the experimental analysis, can make up for the effect of the $P_c(4380)$ in the invariant mass distributions. Of course, the experiment contains and analyzed far more data than the invariant mass distributions, and, in particular, angular correlations are essential to determine the spin-parity of the structures. Yet, whether or not and how possible triangle singularities discussed in Ref. [18, 19] might affect the experimental fits and the determination of quantum numbers are still open questions. An important step towards revealing the exotic nature of the $P_c(4450)$ can be made once they are answered.[5] At last, it is worthwhile to mention that even if it will be shown experimentally that there is a pentaquark state at around 4.45 GeV, the triangle singularity could play a role of enhancing

[4] Sheldon Stone, private communication.

[5] One possibility would be to analyze the data by replacing the resonance parameterization for the $P_c(4450)$ by the amplitudes for the $\Lambda^*\, \chi_{c1}\, p$ triangle diagram as well as other possible triangle singularities discussed in Ref. [19].

the peak signal.

ACKNOWLEDGMENTS

We would like to thank Ulf-G. Meißner and Juan Nieves for comments and a careful reading of the manuscript. This work is partly supported by the Spanish Ministerio de Economia y Competitividad and European FEDER funds under the contract number FIS2011-28853-C02-01, and the Generalitat Valenciana in the program Prometeo II, 2014/068, by the Spanish Excellence Network on Hadronic Physics FIS2014-57026-REDT, by DFG and NSFC through funds provided to the Sino-German CRC 110 "Symmetries and the Emergence of Structure in QCD" (NSFC Grant No. 11621131001), by the Chinese Academy of Sciences (Grant No. QYZDB-SSW-SYS013), and by the Thousand Talents Plan for Young Professionals. FKG and EO would like to acknowledge the hospitality of the Yukawa Institute for Theoretical Physics of Kyoto University and the Institute of Modern Physics of CAS, where part of this work was done.

[1] L. D. Landau, Nucl. Phys. **13**, 181 (1959).
[2] S. Coleman and R. E. Norton, Nuovo Cim. **38**, 438 (1965).
[3] J. J. Wu, X. H. Liu, Q. Zhao and B. S. Zou, Phys. Rev. Lett. **108**, 081803 (2012) [arXiv:1108.3772 [hep-ph]].
[4] X. G. Wu, J. J. Wu, Q. Zhao and B. S. Zou, Phys. Rev. D **87**, 014023 (2013) [arXiv:1211.2148 [hep-ph]].
[5] M. Ablikim *et al.* [BESIII Collaboration], Phys. Rev. Lett. **108**, 182001 (2012) [arXiv:1201.2737 [hep-ex]].
[6] F. Aceti, W. H. Liang, E. Oset, J. J. Wu and B. S. Zou, Phys. Rev. D **86**, 114007 (2012) [arXiv:1209.6507 [hep-ph]].
[7] M. Mikhasenko, B. Ketzer and A. Sarantsev, Phys. Rev. D **91**, 094015 (2015) [arXiv:1501.07023 [hep-ph]].
[8] F. Aceti, L. R. Dai and E. Oset, arXiv:1606.06893 [hep-ph].
[9] C. Adolph *et al.* [COMPASS Collaboration], Phys. Rev. Lett. **115**, 082001 (2015) [arXiv:1501.05732 [hep-ex]].
[10] Q. Wang, C. Hanhart and Q. Zhao, Phys. Lett. B **725**, 106 (2013) [arXiv:1305.1997 [hep-ph]].
[11] N. N. Achasov, A. A. Kozhevnikov and G. N. Shestakov, Phys. Rev. D **92**, 036003 (2015) [arXiv:1504.02844 [hep-ph]].
[12] I. T. Lorenz, H.-W. Hammer and U.-G. Meißner, Phys. Rev. D **92**, 034018 (2015) [arXiv:1506.02282 [hep-ph]].
[13] A. P. Szczepaniak, Phys. Lett. B **747**, 410 (2015) [arXiv:1501.01691 [hep-ph]].
[14] A. P. Szczepaniak, Phys. Lett. B **757**, 61 (2016) [arXiv:1510.01789 [hep-ph]].
[15] X. H. Liu, M. Oka and Q. Zhao, Phys. Lett. B **753**, 297 (2016) [arXiv:1507.01674 [hep-ph]].
[16] R. Aaij *et al.* [LHCb Collaboration], Phys. Rev. Lett. **115**, 072001 (2015) [arXiv:1507.03414 [hep-ex]].
[17] R. Aaij *et al.* [LHCb Collaboration], Chin. Phys. C **40**, 011001 (2016) [arXiv:1509.00292 [hep-ex]].

[18] F.-K. Guo, U.-G. Meißner, W. Wang and Z. Yang, Phys. Rev. D **92**, 071502 (2015) [arXiv:1507.04950 [hep-ph]].
[19] X. H. Liu, Q. Wang and Q. Zhao, Phys. Lett. B **757**, 231 (2016) [arXiv:1507.05359 [hep-ph]].
[20] R. Aaij *et al.* [LHCb Collaboration], Phys. Rev. Lett. **117**, 082003 (2016) [arXiv:1606.06999 [hep-ex]].
[21] R. Aaij *et al.* [LHCb Collaboration], JHEP **1407**, 103 (2014) [arXiv:1406.0755 [hep-ex]].
[22] F.-K. Guo, U.-G. Meißer, J. Nieves and Z. Yang, arXiv:1605.05113 [hep-ph].
[23] F. Aceti, J. M. Dias and E. Oset, Eur. Phys. J. A **51**, 48 (2015) [arXiv:1501.06505 [hep-ph]].
[24] K. A. Olive *et al.* [Particle Data Group], Chin. Phys. C **38**, 090001 (2014).
[25] M. Bando, T. Kugo, S. Uehara, K. Yamawaki and T. Yanagida, Phys. Rev. Lett. **54**, 1215 (1985).
[26] J. J. Wu, R. Molina, E. Oset and B. S. Zou, Phys. Rev. Lett. **105**, 232001 (2010) [arXiv:1007.0573 [nucl-th]].
[27] T. Uchino, W. H. Liang and E. Oset, Eur. Phys. J. A **52**, 43 (2016) [arXiv:1504.05726 [hep-ph]].
[28] P. Fernandez de Cordoba, Y. Ratis, E. Oset, J. Nieves, M. J. Vicente-Vacas, B. Lopez-Alvaredo and F. Gareev, Nucl. Phys. A **586**, 586 (1995).
[29] S. R. Beane, E. Chang, S. D. Cohen, W. Detmold, H.-W. Lin, K. Orginos, A. Parreño and M. J. Savage, Phys. Rev. D **91**, 114503 (2015) [arXiv:1410.7069 [hep-lat]].
[30] L. Roca and E. Oset, arXiv:1602.06791 [hep-ph].